

Failure of a 30 inch diameter oil pipeline due to atmospheric corrosion

Birkitt Keith, Science Division, Health and Safety Executive, UK

Hobbs James, Science Division, Health and Safety Executive, UK

Chapman Ian, Chemicals, Explosives and Microbiological Hazards Division, Health and Safety Executive, UK

Abstract

Ageing pipework across the oil and gas industries are a well-known challenge with significant risks for onshore and offshore operators. From the materials point of view, the common threats are corrosion, erosion, fatigue or materials cracking. Materials degradation can be controlled relatively well assuming detailed knowledge of the processes and original conditions of the materials. Lack of data, process changes or repairs often lead to health, safety and business risks due to unpredictable failures.

In recent years the UK Health and Safety Executive have investigated a number of failures in offshore and onshore pipework. This paper describes an incident investigation following a catastrophic failure in which 208 m³ of light crude oil was released from a pipeline that had deteriorated due to atmospheric corrosion.

An investigation was carried out on a four metre length removed from the pipeline. The investigation utilised optical microscopy, mechanical testing and laser scanning techniques to identify and characterise the material of construction and wall thinning.

The pipeline material was confirmed to be compliant with API 5L grade B steel. The pipeline wall thickness loss was found to be due to atmospheric corrosion of the underside of the pipeline, which was exacerbated by vegetation creating a moist environment. The corrosion developed in a longitudinal pattern over a significant length on the underside, and was accelerated because of debris and close proximity to adjacent pipe runs

Finite element analysis identified that the minimum wall thickness for failure to occur was a fraction of a millimetre and that leak before break would occur, however this was not detected during service and a significant rupture occurred at the head pressure of 2 to 3 barg.

A review of the pipeline inspection regime found a number of failings and recommendations to improvement were made and implemented.

The inspection process identified potential localised corrosion due to debris and vegetation build-up. The consequence of failure was assessed by the operator as a pin-hole leak typically associated with localised external corrosion, so further inspection or remediation was deemed not urgent. The pipeline failed due to a large rupture caused by wall thinning over a significant length, and not pin-hole or leak. It was concluded that the pipeline was not maintained in accordance with the environmental conditions assumed by the applied risk-based inspection regime.

Keywords

Atmospheric corrosion; hydrocarbon pipeline; Finite element analysis; Failure investigation; API 5L B steel.

Introduction

Asset Integrity

Onshore carbon steel pipe networks are subject to a number of internal and external corrosion degradation mechanisms. External corrosion mechanisms include general atmospheric corrosion (in particular at coastal regions and locations with high levels of industrial pollution), crevice corrosion (e.g. under pipe supports), galvanic corrosion and corrosion under insulation (CUI). Internal corrosion mechanisms include erosion-corrosion, galvanic corrosion, CO₂ corrosion, stress corrosion cracking (SCC) and microbiological corrosion (MIC). Each mechanism requires specific conditions for the corrosion to occur.

Understanding the various mechanisms, identifying and implementing inspection and monitoring strategies is key to successful asset management. Failure to adopt a suitable asset management strategy can result in catastrophic releases with highly damaging consequences including loss of production, reputational damage, death, severe injury and ill health to employees and neighbours, and significant environmental damage.

Atmospheric Corrosion

Atmospheric corrosion is well documented and is often not difficult to see, however it still remains as a significant failure mechanism. Carbon and low alloy steels are particularly susceptible to atmospheric corrosion if not adequately protected and/or subjected to suitable inspection regimes. Often the issue is “under the nose” of the operating organisation and yet remains undetected. An assumption that all is well coupled with key visual features such as rust staining - “the pipe has always looked like that” can lead to the pipework being overlooked.

API 571 “Damage Mechanisms Affecting Fixed Equipment in the Refining Industry”, section 4.3.2. [1] identifies a number of typical conditions for the occurrence of atmospheric corrosion:

- Physical location: industrial, coastal, proximity to plant and equipment releasing high volumes of water vapour
- Naturally high humidity
- Elevated temperatures up to 250 °F (120 °C)
- Localised airborne pollutants, e.g. chlorides, H₂S, CO₂, SO₂ etc.
- Bird droppings

Other factors that can affect the corrosion of metallic installations are:

- Poor quality or poorly maintained paint work
- Low temperature pipework inducing condensation
- Temperature cycling
- Orientation to the prevailing wind and rain
- Dissimilar metal connections that can set up a voltaic (galvanic) cell, in which one metal corrodes preferentially to the other when in contact with an aqueous medium.

According to Shreir [2], corrosion rates in the UK can be of the order of 0.048 to 0.170 mm/year depending on location, see Table 1

Table 1 UK atmospheric corrosion rates of mild steel exposed outdoors in different climates [2, 3]

Type of atmosphere	Corrosion rate (mm/year)	Mean corrosion rate (mm/year)
Rural or suburban	0.048 – 0.070	0.062
Marine	0.053 – 0.079	0.066
Industrial	0.095 – 0.170	0.132

The results show the effect of industrial and marine environments over rural or suburban environments and the effect of dry climates over humid/wet climates. However, according to Shreir [2], the corrosion rates in a hot dry desert location may be influenced by other factors such as cold night-time temperatures (and hence condensation) and the salt content of fine wind-blown sand (Awad et al [4]).

The orientation of the metal surface can also have a significant effect on the corrosion rate. According to Shreir [2], tests at Derby in the UK by Dearden, J. [5] showed that specimens exposed at 45° to the horizontal corroded up to 20% more than vertical specimens and that slightly greater than 50% of the total loss was on the underside. Similar tests in the USA by Larrabee, C.P. [6] orientated at 30° to the horizontal, 60% of the metal loss was on the underside. Tests done near the sea at Kure Beach, California, USA, by Laque, F.L. [7] showed a variation by a factor of five depending on the orientation and degree of shelter. The upper surface of a metal will be exposed to the drying effects of the sun and wind, whereas the underside will be less so.

Inspection and monitoring

The corrosive attack can be general or localised depending on the conditions at the site. The degree of metal loss may not be apparent, however red (rust) scale is a key visible indicator. Visual examination is the primary inspection technique supplemented by ultrasonic thickness testing in areas showing signs of corrosion. Full area scanning by phased array would be preferable to spot examination, which may exclude areas of localised wall thinning, especially if a grid system of spot measurements is used. Long range UT can be used to monitor for wall thickness loss, however such systems need to be installed from the outset and can only be applied to straight lengths of pipework.

Onshore Incident

This work describes the investigation of an incident that occurred at a UK refinery installation, in which there was a loss of containment of approximately 208 m³ of light crude oil from a 30 inch nominal bore (NB) pipe section. The failed pipeline was used to transfer light crude from a storage tank via pumps to a crude oil blend tank and onto the processing plant. The location of the pipe failure was within the pump suction pipework and therefore it is believed that it was only subject to an operational head of approximately 2 to 3 bar. The failed section of pipeline was in close proximity to an adjacent insulated refrigerated pipe.

Methodology

Visual examination

The failed pipe is shown in-situ in Figure 1.



Figure 1 Location of incident and non-incident pipe sections

A four metre length of the pipe around the failure location was removed and decontaminated to remove most of the oil residues. Visual and dimensional examinations were carried out before longitudinal sectioning of the pipe section at the 3 o'clock and 9 o'clock positions to create two half-sections – a top half and a bottom half. After sectioning, the pipe was photographed and visually inspected before measuring the pipe wall thickness by laser scanning.

Materials analyses

A sample from the failed pipe was analysed using Inductively Coupled Plasma Optical Emission Spectroscopy (ICP OES) and Combustion to assist in determining the grade of the pipe material. Internal deposits and corrosion products from the incident pipe were analysed using Scanning Electron Microscopy (SEM) and Energy Dispersive X-ray (EDX) analysis.

To assist with the failure analysis, sections were cut from the burst region, and remote from the failure for comparison purposes. The sections were cut and mounted in resin and polished to a one micron finish. The metallographic samples were examined using light microscopy at up to x500 magnification before and after etching in 2% nital.

Hardness tests were conducted on the metallographic samples using a calibrated Vickers diamond hardness testing machine with an accuracy of $\pm 3\%$, and in accordance with BS EN ISO 6507, Parts 1 [8] and 4 [9]. The average hardness value was converted to an approximate ultimate tensile strength in accordance with BS EN ISO 18265 [10].

To assist with the finite element analysis and materials characterisation, two tensile tests were taken from the pipe to obtain the stress strain curves, yield strength and ultimate tensile strength.

Laser scanning

Laser scanning was conducted using an integrated laser scanner on a Romer Absolute arm on the two half-sections of pipework to assess the corrosion pattern and to conduct wall thickness measurements. Measurements were conducted using Polyworks 2018 software. Two areas, approximately 800 mm long from the top and bottom of each pipe were identified for laser scanning. Pipe sections were reconstructed to show visual colour contour maps. Longitudinal and circumferential reconstructions were generated, with measurements, to show the extent of wall thinning.

Finite Element Analysis

Finite element analysis in accordance with API 579 [11] using the limit load approach was used to ascertain the minimum wall thickness for failure to occur and identify whether a leak before break scenario was possible.

Results

Visual examination

The pipe had failed on the underside as shown in Figure 2. The failed pipe section shows minimal protective paintwork and general corrosion of the external surface, Figure 3. The fractured region appeared to be considerably thinner than the general wall thickness, which was approximately 9.5 mm thick. The internal surface of the pipe showed minimal corrosion and the original mill scale from the manufacturing process was still clearly visible, Figure 2. On closer inspection a number of small perforations of the order of a millimeter in diameter were visible.

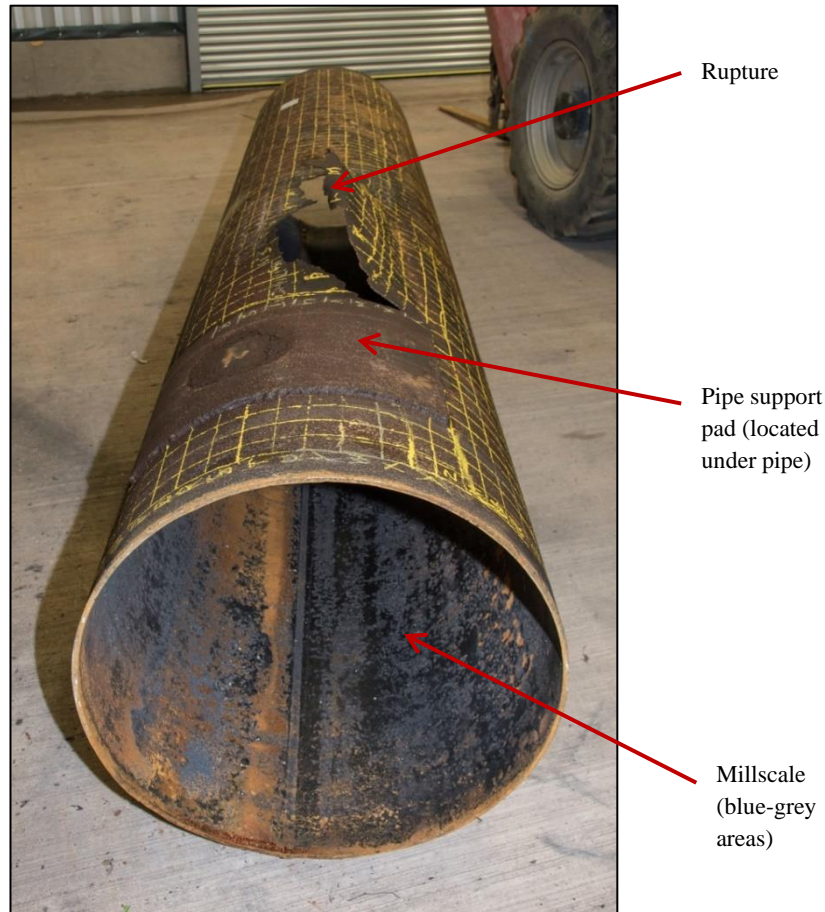


Figure 2 Failed pipe section as received. Note: pipe is shown upside down

Materials analyses

Results of the chemical analysis of the pipe sections material determined by ICP-OES and combustion are given in Table 1. The material was consistent with low-carbon manganese steel, which complied with the composition of API 5L grade B [12] also included in Table 2.

Table 2 Chemical analysis of the incident and non-incident pipes in mass %.

<i>Element</i>	<i>Incident pipe</i>	<i>API 5L grade A [12]</i>	<i>API 5L grade B [12]</i>
Carbon	0.18	Max 0.21	Max.0.26
Silicon	0.03	-	-
Manganese	0.68	Max 0.90	Max.1.15
Phosphorous	0.043	Max. 0.04	Max. 0.04
Sulphur	0.042	Max. 0.05	Max. 0.05
Nickel	0.02	-	-
Chromium	0.04	-	-

Note: if the likely error of the phosphorous analysis (0.03%) is taken into account, then the chemical analysis can be considered to be compliant with both API 5L grade A and API 5L grade B.

The metallographic section remote from the failure revealed external thinning, Figure 3a, with evidence of shallow pitting corrosion, Figure 3b. The microstructure of the pipe consisted of ferrite with small islands of pearlite, consistent with the chemical analysis.

The metallographic section through the failure region revealed a perforation through the wall, Figure 4, and an adjacent area of wall thinning that measured 0.04 mm, Figure 5. The measurement was made using a Mitutoyo traversing microscope with calibrated micrometer scales.

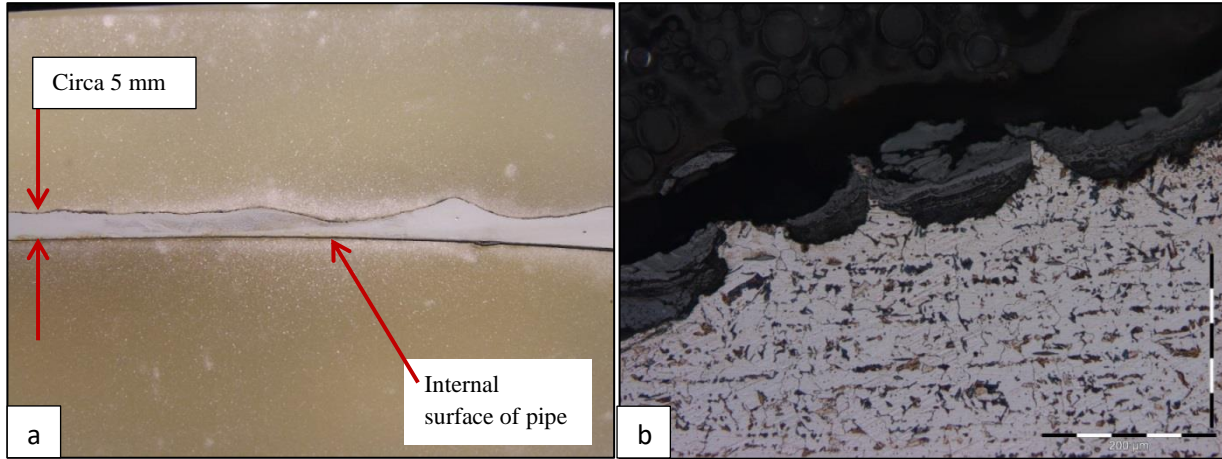


Figure 3 Metallographic sample remote from the failure showing general thinning (a) and external surface corrosion pitting and ferrite/pearlite structure (b)

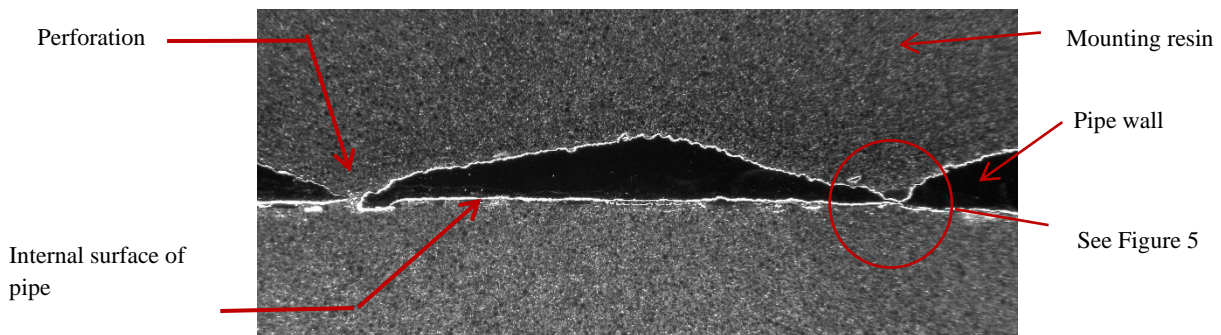


Figure 4 Metallographic section through failure region showing wall thinning away from the burst. The left-hand thinned region has perforated the wall and the right-hand thinned region is 0.04 mm thick.

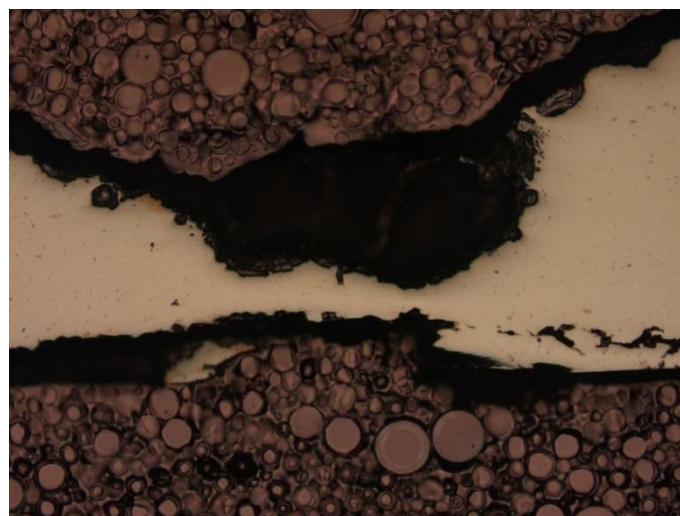


Figure 5 Metallographic section of area circled in Figure 4. Approximate magnification $\times 100$

Hardness tests were conducted on the parent metal of one of the metallographic samples taken close to the failure region. The hardness tests were conducted in accordance with BS EN ISO 6507, Parts 1 [8] and 4 [9]. The measurement accuracy was $\pm 3\%$. The results were 122, 122 and 124 HV10, which gave an average of 123 HV10. When converted to an approximate equivalent tensile strength [10] the result, 410 N/mm², was reasonably consistent with the tensile test results of 454 and 451 N/mm². The results indicated that there was no significant change in mechanical properties within the corroded region. These values were in agreement with the material specification for API 5L grade B [12].

A sample was cut from the end of the pipe section remote to the failure at its thickest location for tensile testing to provide data for finite element modelling. The tensile tests were cut in the longitudinal direction. The tensile tests were conducted in accordance with BS EN ISO 6892 [13] and the results are summarised in Table 3.

Table 3 Tensile test results

<i>Sample ID</i>	<i>0.2% Proof Stress (N/mm²)</i>	<i>Tensile Strength (N/mm²)</i>	<i>Elongation (%)</i>	<i>Reduction of area (%)</i>
J1213	279	454	34	64
J1214	280	451	35	67
<i>API 5L grade A</i>	207 min	331 min	19 min	-
<i>API 5L grade B</i>	241 min	413 min	16 min	-

The results showed that the pipe material was of relatively low strength and consistent with the chemical analysis and hardness. The results are compliant with what would be expected of an API 5L grade A pipe and a grade B pipe. In the author's opinion, in view of the tensile strength and yield strength values obtained, it is likely that the pipe was made to API 5L grade B rather than grade A.

SEM Fractography

Approximately 200mm of the fracture was cut from the ruptured area. This sample was then cut into three pieces and was examined in the scanning electron microscope (SEM). Although the fracture surface was corroded, areas of micro-void coalescence and elongated micro-void coalescence, Figure 6, were visible indicating that the failure mode was ductile tensile overload and ductile shear.

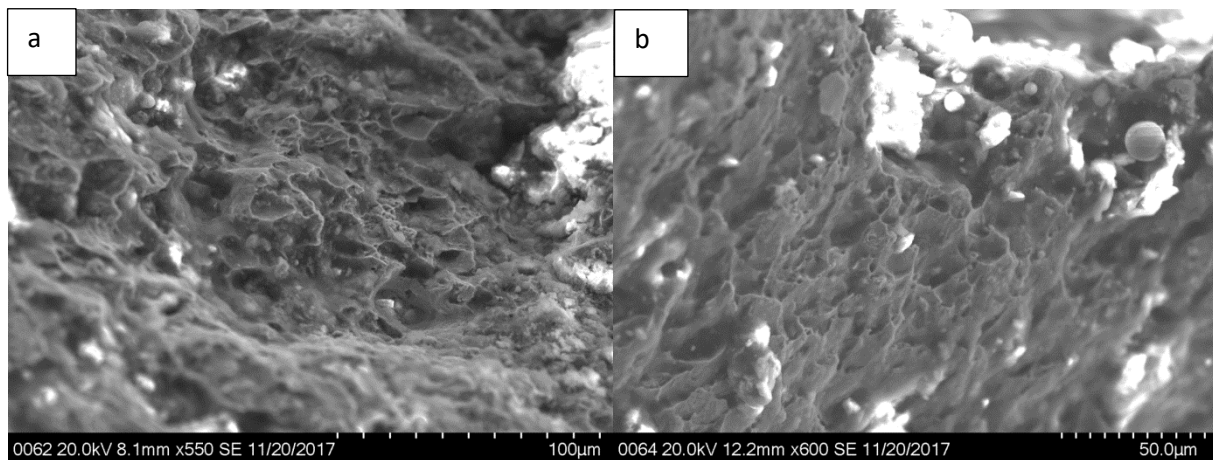


Figure 6 Micro-void coalescence on fractured pipe wall (a) and elongated micro-void coalescence on fractured pipe wall (b)

The internal scale, parent metal and external oxide were analysed using the SEM X-ray analysis facility (EDX). The SEM EDX facility is semi-quantitative and therefore the analyses may not add up to 100% due to rounding errors. EDX analyses involving light elements such as carbon and nitrogen are inaccurate and they are therefore excluded from the results. All analyses contained minor traces of other elements, which for simplicity are not reported in the summary tables. The summary results are given in Table 4.

Table 4 SEM EDX Analysis of pipe material, internal scale and external oxide (mass%)

<i>Analysis ref no.</i>	<i>Location</i>	<i>O</i>	<i>S</i>	<i>Cl</i>	<i>Mn</i>	<i>Fe</i>	<i>Mo</i>
1	Internal scale	17.9	-	-	0.6	81.5	-
2	Internal scale	17.2	0.3	-	0.6	81.9	-
3	Parent metal	-	-	-	0.8	99.2	-
4	Parent metal	-	-	-	0.8	99.2	-
5	External oxide	29.6	-	1.4	0.3	68.8	-
6	External oxide	30.2	-	0.5	-	68.7	0.6

The results in Table 4 showed that the SEM EDX analysis of the parent metal was consistent with the OES analysis, The internal scale was likely to be mill scale with a small amount of sulphur from the oil/gas and that the external scale contained some chlorine, consistent with a coastal location.

Further detailed analysis was conducted of the external corrosion products close to the pipe rupture and the average results for three areas are given in Table 5.

Table 5 Average SEM EDX results of external surface adjacent to pipe rupture (mass %)

Location	O	Na	Al	Si	P	S	Cl	K	Ca	Mn	Fe
Area 1	29.7	0.7	2.0	1.6	0.1	6.3	0.3	0.3	0.8	0.3	57
Area 2	29.7	1.1	1.5	1.4	-	4.5	-	0.1	1.3	0.4	57
Area 3	36.3	3.6	0.5	2.7	0.2	0.2	1.8	1.6	2.0	0.5	49

The results showed that the pipe external surface consisted of an oxide of iron (containing iron, manganese and oxygen) with traces of sodium, aluminium, silicon, sulphur, chlorine and calcium. The sodium and chlorine were probably due to presence of sodium chloride in the coastal environment. The sulphur was probably from the oil within the pipe. The source of calcium is believed to be from an adjacent chalk bank.

Laser scanning

Internal and external laser scanning of the pipe was conducted to ascertain the degree and location of wall thinning. General colour profile maps of the top and bottom halves are shown in Figures 7 and 8. Eight circumferential line scans and four longitudinal line scans with spot measurements were taken and an example is shown in Figure 9.

The colour profile maps clearly show that significant external thinning of the pipe wall had occurred at the 4 to 8 o'clock positions with the greatest wall thinning to less than 2.5 mm at the 5 to 7 o'clock positions. The line scans show significant external wall thinning to less than 2 mm away from the burst. In the vicinity of the burst, the scans indicate that thinning to less than 1 mm had occurred. On one of the longitudinal line scans, adjacent to the burst, an area of wall thinning was measured and found to be 0.4 mm, which corresponds to the approximate location of the pin holes observed.

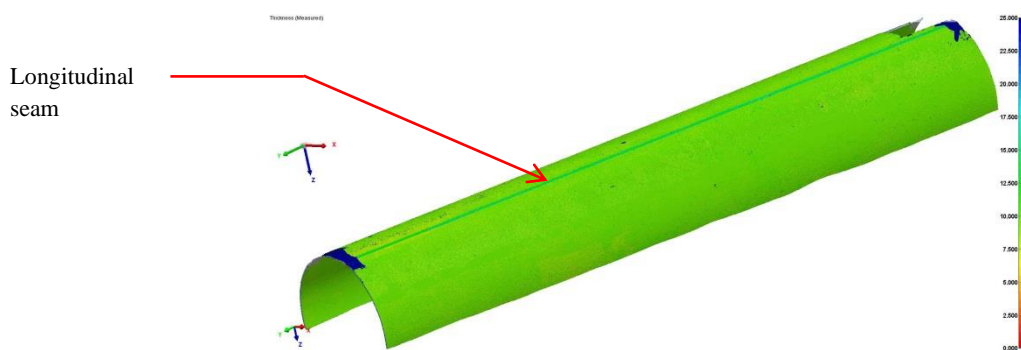


Figure 7 Laser scan colour profile map of topside of pipe showing longitudinal seam and uniform thickness

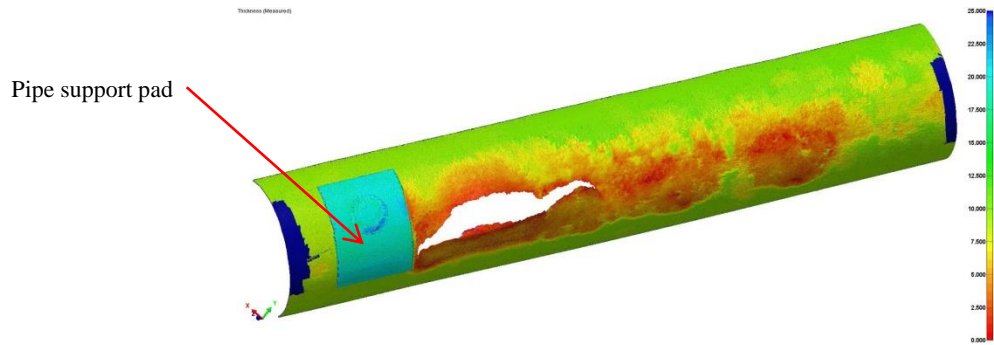


Figure 8 Laser scan colour profile map of underside of pipe showing thinning in yellow, orange and red

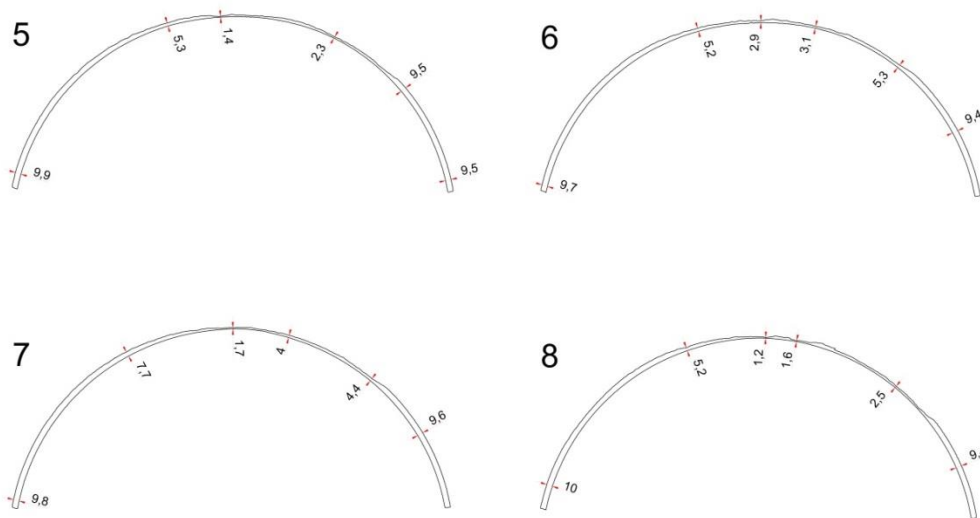


Figure 9 Example of laser line scans of lower half of pipe away from burst

Finite Element Analysis

Geometry

Attempts were made to use the laser scan data from the actual pipe for the modelled geometry. There were a number of difficulties with this approach:

- The actual rupture location was highly distorted and did not represent the condition before rupture
- The internal surface of the pipe was only scanned after sectioning of the pipe, which resulted in some movement. This made matching the scanned data to the original diameter difficult for areas away from the rupture
- The detailed surface geometry obtained from the scan resulted in difficulties meshing

Therefore, an idealised geometry was created. This approach avoided the problems listed above and enabled different types of thinning to be assessed. The dimensions of the section of pipe modelled were length of 1 m, outside diameter of 760 mm, and a nominal thickness of 10 mm.

The thinning was achieved using an intersecting arc removing material from the outer surface, as shown schematically in Figure 10a. The axial length of the thinned region was 850 mm. Using an arc of radius 400 mm resulted in a circumferential extent of 316 mm to the thinned area. The model was a quarter model, with symmetry planes in the vertical axial plane and the transverse plane at the thinned end.

Therefore, the dimensions quoted represent half of the full lengths of the thinned region. Using this method, the pipe was thinned to remaining ligament thicknesses of 1 mm and 0.75 mm.

Further reductions to the thickness were achieved by subtracting a cylindrical volume of material (length = 60 mm, radius = 1.75 mm), as illustrated in Figure 10b. A local thinned area down to 0.25 mm was obtained using this method. Within this locally thinned section, some perforations were added, as shown in Figure 11, by subtracting spheres with a diameter of 2 mm.

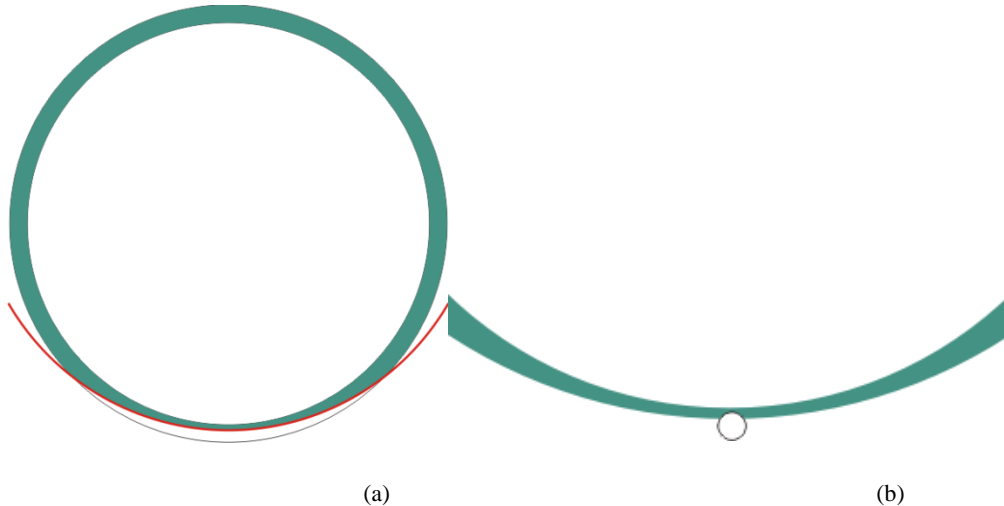


Figure 10 Schematic diagram illustrating methods of general thinning (a) and local thinning (b)

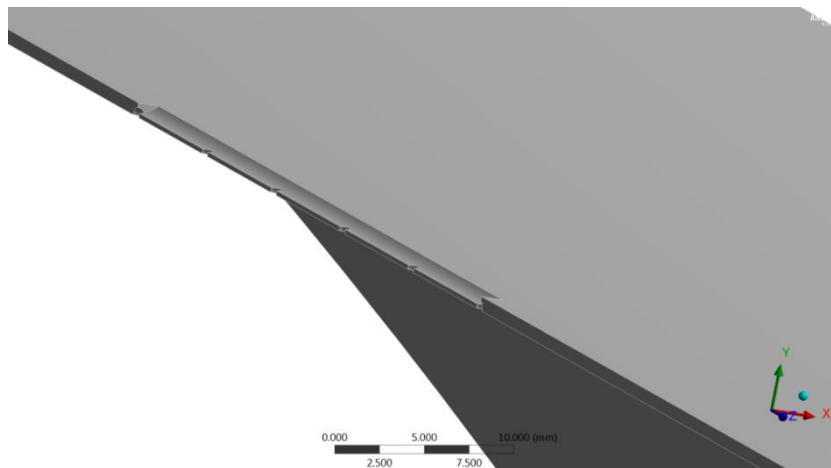


Figure 11 Locally thinned area (down to 0.25 mm) within generally thinned area (0.75 mm)

Loading and Boundary Conditions

Symmetry constraints were applied to the surfaces on the longitudinal/vertical plane, and the transverse plane at the thinned end of the modelled section.

Pressure loading was applied to the internal surface of the pipe. The magnitude of the pressure was gradually increased until the model failed to converge to a solution.

Material Properties

A simple elastic-perfectly plastic material model was used, with the yield stress set to 285 MPa, as obtained from tests of the pipe material. This may be higher than the minimum specified for the material that would be used in design or fitness-for-service calculations.

Results

The assessment method was based on the API 579 [11] Limit Load approach. This approach uses an elastic-perfectly plastic material model and defines the limit load as the maximum load (or pressure) at which the model converges to a solution. As it takes no account of strain hardening, it will provide a lower bound estimate of the actual failure pressure. It should be noted that this approach is not accepted

in BS 7910 [14], as the convergence of the model is dependent on the model details (such as mesh quality and size of the loading increments).

The assessments were a (lower bound) prediction of burst pressures, not full fitness-for-service assessments (such as to API 579 or BS 7910). There may be criteria, such as minimum thickness ratios, or minimum thicknesses, that would deem the pipe to be unacceptable in its thinned state that have not been assessed here.

The main results for the three models are listed in Table 6.

Table 6 Main results

Model	Maximum pressure† (bar)
General thinning to 1 mm	8.5
General thinning to 0.75 mm	6.4
General thinning to 0.75 mm with local thinning to 0.25 mm and perforations	2.4

†Maximum pressure at which solution converged for the perfectly plastic model.

Actual failure pressure likely to be higher

The operating pressure is understood to be between 2 bar and 3 bar. The results show that in the absence of higher pressures, the pipe would need to be thinned to well below 1 mm to burst.

The geometries modelled have been simplified; different thinning geometries (such as different lengths or shapes or local thinning) may have produced different results. However, from the results obtained, it is clear that some areas of very low thickness would be required for the pipe to fail.

It is clear that the pipe wall would have to corrode significantly before bursting. It is highly likely that some points on the surface would corrode more than others, possibly resulting in either pinholes or very local failure resulting in leakage. However, this does not automatically imply that a leak-before-break case can be made. A formal leak-before-break case (for example, based on BS7910) would require it to be demonstrated that a leak *must* occur before burst, and that any leak would be detected before sufficient further degradation could occur to cause a burst. This would involve calculation of the leak rate and establishing the sensitivity of leak detection/inspection systems. While it may be straight-forward to demonstrate that a crack would grow to be through wall before reaching a critical length, demonstrating that an unpredictable pattern of corrosion could not form into a shape that could cause a burst may be more difficult.

Similarly, it is not clear whether a detectable leak would have been present in the incident pipe. It is not possible to determine whether the rupture in the pipe occurred in one event, or started with a local leak. Some pinholes were observed when the pipe was examined in the laboratory, but such small holes could have been blocked with contamination or corrosion products. Vegetation growing around the area of the rupture would also make detecting a small leak more difficult.

Discussion

The pipe had been manufactured from C-Mn steel, which was compliant in so far as tested, with API 5L grade B with a tensile strength of 450 N/mm², a yield of 280 N/mm² and an elongation of 34%.

The pipe appeared to have had an original wall thickness of approximately 10 mm. Laser scanning revealed large areas of significant external wall thinning on the underside of the pipe between the 4 and 8 o'clock positions. The greatest wall thinning, below 2.5 mm, was evident at the 5 to 7 o'clock positions. Examination of the pipe in-situ and examination of the sample retrieved showed that the pipe was largely un-painted, or rather that the original paint layer had weathered and corroded away.

A few millimetres away from the rupture, the pipe wall thickness was approximately 1 mm. At the point of fracture the wall thickness was well below 1 mm. On a metallographic cross section adjacent to the fracture, a section of wall was measured and found to be 0.04 mm. The area of the very thin wall at this location was quite small and was surrounded by thicker material. Examination of the fracture surface showed it to be a ductile shear failure with a small region of ductile tensile failure, caused by a localised overpressure as a result of wall thinning.

SEM EDX analysis showed traces of chlorine on the external corrosion deposits. The source of chlorine was probably due to chlorides from the coastal atmosphere. The moist coastal air containing sodium chloride would have accelerated corrosion when compared to an inland location. According to published data [2, 3] the corrosion rate of unprotected mild steel in a coastal environment would be of the order of 0.05 to 0.08 mm/year. At these corrosion rates, to obtain a wall thickness below 1 mm would require 110 to 180 years. Clearly,

there would need to be another factor to obtain a faster corrosion rate. According to the investigation team, there was a bank containing chalk adjacent to the pipe and this bank had exhibited subsidence and erosion. The presence of calcium in the external deposits may be contamination from the eroded and weathered chalk bank.

From photographs taken on site, there was significant vegetation present. During autumn and winter, leaves shed from shrubs could accumulate between the incident pipe and the adjacent lagged pipe and would provide an organic matt, which could aid corrosion. According to Shreir [2], dead organic matter may render water corrosive by making it acidic. The proximity of the bushes would also prevent the free movement of air underneath the pipe, which would increase the local humidity and allow the pipe to remain wet for longer periods of time.

The under-side corrosion is explained by the proximity of the adjacent pipes and vegetation. Corrosion rate differences according to orientation of the corroded item have been observed [2, 5, 6, 7]. Had the pipe been maintained by the application of protective layers of paint, then corrosion could not have occurred.

According to on-site investigators, the adjacent pipe work was clad with aluminium shielded lagging. Consideration of the galvanic series [15] shows that aluminium would corrode preferentially to the steel. Therefore, it is highly unlikely that the presence of the adjacent pipe would contribute to corrosion of the pipe by a galvanic corrosion mechanism, and this was not observed in the corrosion pattern seen on the laser scans.

Finite element modelling of the rupture indicated that wall thinning well below 1 mm was necessary for failure to occur and this was found to be the case with regions as thin as 0.4 mm on the laser scan and 0.04 mm on one of the metallographic sections.

With such a degree of thinning required to cause failure, it is likely that leak would occur before rupture. However, this does not necessarily mean that a leak-before-break case could be made, which would have to show that a leak must occur before rupture, and that any leak would be detected. Also, it is not certain that a detectable leak occurred in the incident pipe before rupture. Although pinholes were found, it is possible that these were blocked with corrosion product, preventing leakage. The vegetation in the area would also make inspection and detection of any leak more difficult.

Following the incident, the duty holder undertook a review of the maintenance and inspection regime and concluded:

- There was an assumption made when viewing the inspection reports that the likely failure mode would be a pin hole leak or potentially a small leak hole as predicted within the Risk Based Inspection (RBI) program for atmospheric corrosion. In the event the linear corrosion pattern due to proximity of the other line and soil build up had not been adequately considered within the review of the inspection report. One improvement was to ensure that such situations are adequately validated to ensure degradation patterns are as expected.
- There was a need to ensure equipment was operated within the assumptions within the RBI program, therefore a major exercise was launched that looked to clear pipe tracks of soil build up and vegetation and identify other areas where there may be elevated risk of deviation such as poor clearance between pipework etc within the pipe tracks.

Conclusions

The pipe had been manufactured from C-Mn steel compliant, in so far as tested, with API 5L grade B with a tensile strength of 450 N/mm², a yield of 280 N/mm² and an elongation of 34%.

The pipe appeared to have had an original wall thickness of approximately 10 mm. Laser scanning showed significant external corrosion, which had reduced the pipe wall to below 2.5 mm on the underside of the pipe. Localised wall thinning down to 0.4 mm was found, with wall thinning down to 1 mm approximately 5 mm away from the rupture.

The finite element model predicted that failure would occur if the pipe wall thickness was well below 1 mm. Therefore, it is likely that leak would occur before rupture. However, this does not necessarily mean that a leak-before-break case could be made, which would have to show that a leak must occur before rupture, and that any leak would be detected.

The failure mode was a combination of ductile tension and ductile shear.

Around the fracture there were traces of chlorine, which were probably due to the coastal location. The moist coastal air would have accelerated corrosion when compared to an inland location.

The affected length of pipe was devoid of a protective paint layer.

The proximity of an adjacent pipeline and vegetation would have assisted with creating a damp atmosphere beneath the pipe, promoting corrosion. As the adjacent pipe was reported to be almost touching the corroded pipe, decaying vegetation could have accumulated in the gap between the two pipes and provided a more corrosive environment.

In summary, the pipe failed due to external corrosion, which reduced the wall thickness to below 1 mm and to a thickness that could no longer withstand the internal pipe pressure, at which point ductile rupture occurred.

Recommendations for avoiding atmospheric corrosion of pipework

- Factor into the asset management and inspection regime to periodically visually inspect pipework even if it is assumed to be low risk
- Factor into the asset management regime to routinely clear away accumulating debris and vegetation
- If corroded pipework is found, conduct ultrasound inspection to determine actual wall thickness, paying particular attention to vulnerable areas such as the underside and low points of the pipework system.
- Maintain paintwork in accordance with the original (or a suitably modified) specification
- Adopt an awareness of the risks of purely desk based or remote assumptions when reviewing inspection reports and re-assessing the RBI strategy.
- Ensure that equipment is operated and maintained in accordance with the assumptions contained within the RBI strategies.

References

- 1 API Recommended Practice 571 “*Damage Mechanisms Affecting Fixed Equipment in the Refining Industry*”, 2nd edition, April 2011. American Petroleum Institute. Section 4.3.2.
- 2 Shreir’s Corrosion, Volume 3, “*Corrosion and Degradation of Engineering Materials.*” Section 3.01 Corrosion of Carbon and Low Alloy Steels. 2010.
- 3 “*Sixth Report of the Corrosion Committee*”, Spec. Rep. No. 66, Iron and Steel Institute: London, 1959.
- 4 Awad, G.H.; Abdel Halim, F.M;El Arabi, R.M. British Corrosion. Journal. 1980. 15, 140.
- 5 Dearden, J. Journal of the Iron and Steel Institute. 1948, 159, 241.
- 6 Larrabee, C.P. Transactions of the Electrochemical Society. 1944, 85, 297.
- 7 Laque, F.L. Materials Performance. 1982, 21, 17.
- 8 BS EN ISO 6507- Part 1: 2018, “*Metallic materials. Vickers hardness test- Test Method.*” British Standards Institution.
- 9 BS EN ISO 6507- Part 4: 2018 “*Metallic materials. Vickers hardness test- Table of Hardness values.*” British Standards Institution.
- 10 BS EN ISO 18265:2013, “*Metallic materials-conversion of hardness values.*” British Standards Institution.
- 11 API 579-1/ASME FFS-1 “*Fitness-For-Service*”. June 2016. American Petroleum Institute.
- 12 American Petroleum Institute Standard, API 5L, “*Specification for Line Pipe, API Specification 5L*”, *Iron and Steel Specifications*, 5th edition, November 1979. British Steel Corporation.
- 13 BS EN ISO 6892 -1:2016, “*Metallic materials – Tensile testing, Part 1: Method of test at ambient temperature*”. British Standards Institution.
- 14 BS 7910: 2013 + A1 2015 “*Guide to methods for assessing the acceptability of flaws in metallic structures*”. British Standards Institution.
- 15 ASM Metals Handbook, Ninth Edition, Volume 13.